The Improved H-Mode at ASDEX Upgrade: a Candidate for an ITER Hybrid Scenario

A. Staebler, A.C.C Sips, M. Brambilla, R. Bilato, R. Dux, O. Gruber, J. Hobirk, L.D. Horton, C.F. Maggi, A. Manini, M. Maraschek, A. Mück, Y.-S. Na[+], R. Neu, G. Tardini, ASDEX Upgrade Team.
Max-Planck-Institut für Plasmaphysik, EURATOM Association, 85748 Garching, Germany
[+]Korea Basic Science Institute, 52 Yeoeun-Dong, Yusung-Gu, Daejeon, 305-333, Korea
E-mail: albrecht.staebler@ipp.mpg.de

Abstract. A stationary regime with improved confinement ($H_{98(y,2)}$>1) and, simultaneously, improved stability (β_N>2.5) compared to standard H-mode has been investigated on ASDEX Upgrade for many years. This so-called "improved H-mode" is characterized by a q-profile with low central magnetic shear and $q_0 \geq 1$ that is obtained by early heating during the current ramp. The existence domain of this scenario is documented for $3.2<q_{95}<4.5$ and n_e/n_{GW} up to 0.85. When compared with standard H-mode, core transport is still governed by drift-wave turbulence but stronger peaked density profiles and, possibly, a higher edge stability may be responsible for the increase in confinement. Impurity control is achieved by central wave heating. The improved stability is due to the q-profile: by $q_0>1$ sawteeth as the main trigger of large NTMs are avoided and the low shear significantly reduces the amplitude of (3,2) modes present at high β. The stability is eventually limited by the occurrence of a (2,1) mode at typically $\beta_N \sim 3$. As far as the reactor relevance of this regime is concerned, its compatibility with significant central electron heating, with high edge densities and with type-II ELMs is of importance. The improved H-mode is, therefore, seen as candidate for a long pulse ITER "hybrid" operation.

1. Introduction

ELMy H-modes at high plasma current are foreseen as the standard operation regime of ITER (15 MA at 5.7 T; q_{95} = 3), based on a large experimental data base from many tokamaks. A reference baseline scenario has been defined with a confinement factor $H_{98(y,2)}$ = 1 compared to H-mode scaling [1] at a normalized β value of β_N = 1.8. Advanced scenarios aim at improving confinement and stability above these values in order to operate ITER at reduced plasma current and therefore lower disruption forces and longer pulse lengths at the same performance. This performance can be expressed in terms of $\beta_N \cdot H/q_{95}^2$, a common figure of merit for the fusion gain Q. On ASDEX Upgrade such a regime of stationary operation with $H_{98(y,2)}$ ~ 1.4 and β_N > 2.5, obtained simultaneously at q_{95} ~ 4, has been developed since 1998 [2]. It is called "improved H-mode" and is characterized by a stationary q-profile with $q_0 \geq 1$, but typically close to 1, a low central magnetic shear and the absence of sawteeth. Further developments of this or similar regimes in recent years by ASDEX Upgrade and other tokamaks [3, 4, 5] have been done in order to document the improved H-mode as a candidate for long pulse ITER operation – a "hybrid" of the non-inductive, reversed shear scenario with internal transport barriers (ITB) and the standard H-mode baseline scenario with sawteeth and the usual monotonic q-profile (q_0 < 1). The recent work on ASDEX Upgrade was focussed on the documentation of the existence region of the improved H-mode in q_{95} and density, on the role of the MHD behaviour with respect to stability and stationary conditions, on transport of heat and impurities, and on the demonstration of the improved H-mode with significant central electron heating.

This paper is organized as follows: in section 2, the experimental procedure to obtain the improved H-mode and its main characteristics are described. Section 3 reports the results of the various parameter scans. Plasma profiles and transport analysis including impurity behaviour is discussed in section 4, followed by a description of the MHD observation in this type of discharges (section 5). The existence of improved H-modes in the presence of dominant central ion cyclotron resonance heating (ICRH) is addressed in section 6. The paper ends with a brief summary (section 7).

2. Characterisation of the Improved H-Mode at ASDEX Upgrade

As mentioned above, access to the improved H-mode requires to create and maintain a q-profile with $q_0 \geq 1$ and a low central magnetic shear. By this, sawteeth are avoided which could trigger large amplitude, confinement deteriorating neoclassical tearing modes (NTM). An example of an improved H-mode with $I_p = 1$ MA, $q_{95} = 3.8$, low triangularity ($\delta \sim 0.2$) and moderate density ($n_e/n_{GW} \sim 0.4$) is shown in Fig. 1. The specific q-profile is obtained by early neutral beam (NBI) heating at 0.3 s during the current ramp to reduce the current diffusion, but at a moderate input power (2.5 MW) to avoid the formation of an ITB. The transition from limiter to lower single null divertor configuration takes place at 0.5 s. A later transition to the divertor configuration and a somewhat stronger heating during the limiter phase can be used as an alternative. The NBI power is stepped up to 5 MW at the beginning of the current flat top (t = 1 s), which coincides with the start of the type-I ELMy H-mode phase (see D_α-trace). A recipe to obtain reproducibly high plasma performance is to delay the further power increase by about 1 s, presumably, to allow for an equilibration of the current profile. In the discharge of Fig. 1, the NBI power is increased to almost 10 MW with power ramps produced by on/off-modulation of the beams. After the first ramp β_N rises to a value close to 3, not far from the no-wall limit ($4{\cdot}l_i$). During this ramp the H-factor increases with increasing input power, a fact often observed in improved H-mode discharges. At 4.9 s a small amplitude (3,2) NTM develops (see Fig. 2) which however only slightly affects the confinement. During the further ramp of the heating power a small increase of this activity is observed but β_N remains around 2.8. In this discharge $\beta_N{\cdot}H_{98(y,2)}/q_{95}^2 \sim 0.25$ is maintained for 3.7 s (more than $25{\cdot}\tau_E$) which is to be compared with $\beta_N{\cdot}H_{98(y,2)}/q_{95}^2 \sim 0.2$ for the ITER baseline scenario ($q_{95} \sim 3$).

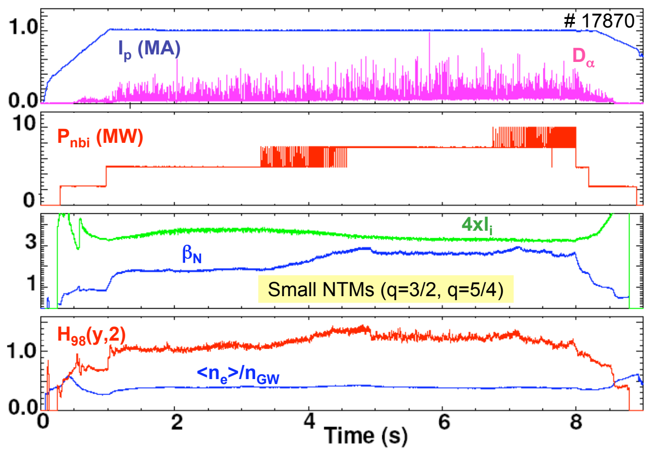

Fig. 1: Time development of plasma parameters for an improved H-mode discharge at q_{95}=3.8.

In addition to the experimental procedure described so far, an adequate choice of the beams is important to reliably access the improved H-mode. Two of the eight ASDEX Upgrade beams are directed to obtain off-axis, tangential injection and in the discharge of Fig. 1 these beams were applied for the power steps to 5 MW and to 7.5 MW, respectively. Recently, off-axis tangential beams are routinely included to obtain improved H-modes [6].

Fig. 2 shows in the upper part a spectrogram of the MHD activity from Mirnov coils for the same discharge as given in Fig.1. After a short (1,1) mode at the beginning of the flat top there is no prominent mode activity seen during the 5 MW heating phase. Following the rise of β_N to close to 3, (5,4) and later (3,2) modes appear with a minor effect on the confinement as shown in Fig. 1. Small amplitude mode activity or fishbones are often observed during the high performance phase in improved H-modes. In the lower part of Fig. 2 the central and minimum q-values obtained from the MSE measurement are compared with the results from

ASTRA [7] simulations which take into account the expected beam driven current density from the off-axis, tangential beams. After the (1,1) mode disappears the measured q_0 (= q_{min}) stays at a constant value above 1 but with no reversal of the q-profile, whereas the simulation results in a drop of q_0 below 1 which is clearly not consistent with the absence of (1,1) activity and sawteeth.

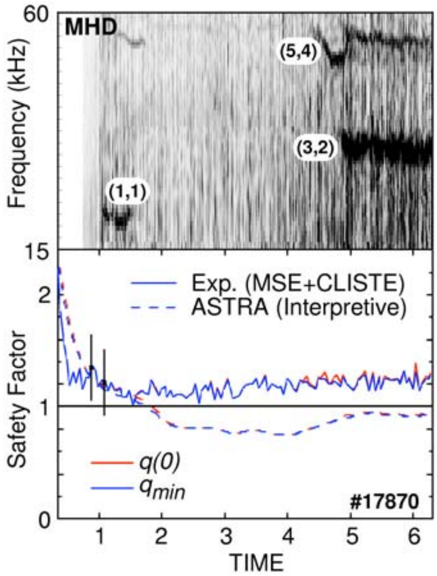

Fig. 2: For shot of Fig. 1; top: spectrogram of MHD activity from Mirnov coils; bottom: q_0 and q_{min} from MSE and ASTRA simulation.

3. Documentation of the Existence Domain of the Improved H-Mode

In order to qualify the improved H-mode as a valid scenario for ITER extensive parameter scans are required. On ASDEX Upgrade, the existence domain of this scenario has been studied by performing scans in q_{95} and density. In addition, discharges have been set up for which ρ^* is varied over the widest possible range under otherwise similar parameters.

A scan in q_{95} was performed at fixed plasma current (I_p = 1 MA) by varying the toroidal field as the H-mode confinement depends only weakly on B_t. Stationary operation of the improved H-mode at high β_N ($\geq$ 2.5) and high $H_{98(y,2)}$ ($\geq$1.1) was documented at three different values of q_{95} (3.3, 3.8 and 4.3). Parameters achieved during the stationary phases are listed in Table I (row #1-4). In this table, ρ_i^* and ν^* are calculated using the volume averaged ion temperature and density, respectively. The density in this scan was kept low (n_e/n_{GW} ~ 0.4, no external gas feed) resulting in a collisionality, ν^*, close to the ITER value (see Table I). At q_{95} = 3.3 sawteeth are not completely suppressed but they are of small amplitude and do not trigger a large amplitude NTM as long as β_N stays below 3. The amount of NBI power that can be applied at q_{95} = 4.3 is significantly higher compared to q_{95} = 3.3, leading to stationary values of $\beta_{pol} \geq 1.5$ at the higher q_{95} ($\beta_N \geq 2.6$). Any attempt to rise β_N above 3 during these experiments leads to the occurrence of "large" (2,1) NTMs with a strong reduction in confinement (see sect. 5). The existence of the improved H-mode over a wide range of q_{95} is important for the extrapolation of this regime to ITER. Improved H-modes at low q_{95} close to the ITER reference value of q_{95} = 3 would allow to exceed the ITER design value of Q = 10 mainly because ITER assumes a conservative β limit at this q_{95} of β_N ~ 1.8. On the other hand, improved confinement and stability at higher q_{95} around 4 offers the possibility to operate ITER at reduced current without a reduction in performance, but having the benefits of longer pulses due to less flux consumption and a higher bootstrap fraction and of a reduced potential for damage in case of a disruption.

Table I: *Improved H-mode parameters from: q_{95} scan (#1-4), high-n_e (#5), ρ_i^* scan (#6, 7). (Values averaged over period with $0.85 \cdot \beta_{N,max} \leq \beta_N \leq \beta_{N,max}$)*

#	I_p (MA)	B_t (T)	q_{95}	dur/τ_E	n_e/n_{GW}	β_N	$H_{98(y,2)}$	ρ_i^*	ν^*/ν^*_{ITER}
1	1.0	1.85	3.31	30	0.38	2.52	1.06	7.8E-03	1.7
2	1.0	2.10	3.82	25	0.41	2.81	1.39	11.4E-03	1.5
3	1.0	2.34	4.26	15	0.41	2.55	1.15	11.3E-03	1.6
4	1.0	2.34	4.25	9	0.45	3.02	1.22	10.7E-03	1.5
5	0.8	1.69	3.61	44	0.85	3.49	1.11	9.3E-03	10.7
6	0.6	1.39	4.19	30	0.56	2.80	1.02	12.8E-03	5.2
7	1.2	2.78	4.19	14	0.52	2.60	1.00	8.2E-03	2.5

The improved H-mode is not restricted to low densities. By carefully adjusting heating power and gas puff rate in a high triangular ($\delta \sim 0.45$) plasma with $q_{95} = 3.6$, improved confinement ($H_{98(y,2)} \sim 1.1$) and stability ($\beta_N \sim 3.5$) could be sustained for up to $45 \cdot \tau_E$ at high densities close to the Greenwald limit ($\langle n_e \rangle / n_{GW} = 0.85$). Further parameters are given in Table I (row #5) and more details of theses high-n_e improved H-modes are reported in refs. [6]. Even though ν^* in these discharges is significantly above the ITER value it is important to realize that high edge densities as required for power and particle exhaust in a reactor and small amplitude type-II ELMs are compatible with the improved H-mode regime.

In view of the unfavourable scaling for the onset of NTMs with ρ^* in standard H-modes, where sawtooth crashes seed the growth of an NTM, the dependence of the improved H-mode performance on ρ^* is an important issue. Discharges have been set up where ρ^* is varied over the widest possible range in ASDEX Upgrade at a fixed shape, $q_{95} = 4.19$ (0.6 MA/1.39 T, 1.2 MA/2.78 T) and $n_e/n_{GW} \sim 0.6$. In both discharges stationary operation at $\beta_N \geq 2.6$ and $H_{98(y,2)} \geq 1.0$ are achieved (see Table I, row #6, 7). The value of ρ^* is lower in the high current discharge by roughly a factor of $\sqrt{2}$, as expected from scaling, with no effect on stability and performance. Further results concerning the ρ^* scaling towards ITER are expected from inter-machine comparisons.

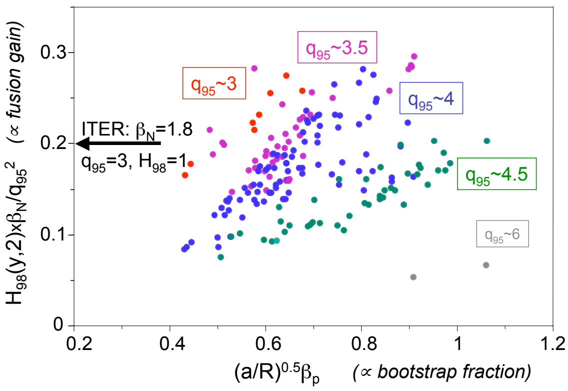

Fig. 3: Performance vs. $\sqrt{\varepsilon} \cdot \beta_p$; data base: all improved H-mode studies in 2003/2004, including low power phases; colour code: q_{95} range.

As a summary of the results obtained during the improved H-mode studies, the achieved performance in terms of $H_{98(y,2)} \cdot \beta_N / q_{95}^2$ is plotted vs. $\varepsilon^{0.5} \cdot \beta_p$ in Fig. 3. The latter quantity is a measure of the bootstrap current. Data are taken from essentially all improved H-mode experiments over the past two years for different time slices during the shots, also at low heating power and different heating methods. Clearly, a high performance was achieved which exceeds the value expected for the ITER baseline scenario for $3 < q_{95} \leq 4$ and reaches this value at $q_{95} \sim 4.5$. For all q_{95} values, stationary long pulses (duration/$\tau_E > 40$) were obtained close to the maximum performance, limited only by technical reasons. Operation at higher q_{95} allows a significant bootstrap fraction to be achieved. In ASTRA simulations of high β_p improved H-modes a non-inductive current fraction of about 50% has been found, mainly due to the bootstrap current [8].

4. Plasma Profiles, Transport Analysis and Impurity Control

The improved confinement with respect to global H-mode scaling rises the question whether the local heat conductivity in the improved H-mode scenario is different from the one in standard H-modes. Heat transport in the latter scenario is determined by the onset of turbulence (ITG, TEM) above a critical value of $\nabla T / T$ [9] resulting in "stiff" temperature profiles, i.e. a fixed ratio between central and edge temperature. In Fig. 4 $T_i(\rho \sim 0.4)$ is plotted vs. $T_i(\rho \sim 0.8)$ for a subset of recent improved H-mode data together with some data from standard H-modes. Clearly, ion temperature profiles in improved H-modes are stiff with the same gradient length as in standard H-modes, confirming the results of an earlier study [10]. A detailed transport analysis of the improved H-mode shown in Fig. 1 based on ASTRA simulations shows that the ion heat transport is still governed by ITG/TEM turbulence in the

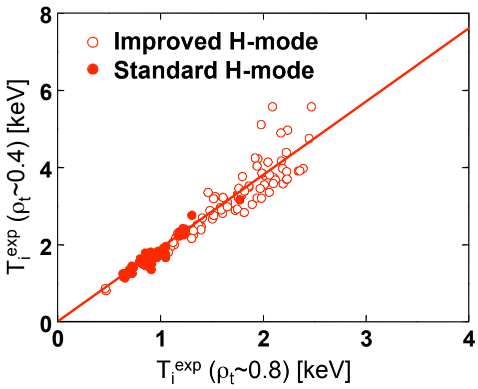

Fig. 4: $T_i(\rho\sim0.4)$ vs. pedestal-T_i for standard and improved H-modes, indicating stiff T_i-profiles.

confinement region [11], in agreement with the observations of stiff ion temperature profiles. A similar conclusion is reported from the analysis of corresponding DIII-D discharges [12]. As far as electron heat transport is concerned, power balance and transient response analysis to modulated electron cyclotron resonance heating (ECRH) of low density improved H-modes were found to be consistently described by a transport model with a threshold in $\nabla T_e/T_e$, above which the electron heat transport is increased [13]. A comparison with pure EC heated L-modes points to a stronger resilience of T_e in the improved H-modes.

In contrast to the temperature profiles, density profiles are not stiff. Improved H-mode discharges are characterized by stronger peaked density profiles compared to normal (sawtoothing) H-modes. This is shown in Fig. 5a where the density peaking, defined as $n_e(0)/n_e(\rho\sim0.9)$, is plotted against the line averaged density for the same improved H-mode data base as given in Fig. 3 and for some representative standard H-modes which comprise a variation of heating method and power, density and q_{95}. The stronger density peaking attainable in improved H-modes is correlated with the lower collisionality due to the higher temperatures, in agreement the findings of Ref. [14]. At fixed temperature profiles, the higher central densities in improved H-modes result in higher stored energies. This can explain to some extent the increase in confinement factor, given in Fig. 5b. Even though the scatter is rather large, the data indicate that the density peaking may not be fully responsible for the improvement in $H_{98(y,2)}$ since even for $n_{e,0}/n_{e,ped} \leq 2$ higher H-factors for improved H-modes are found compared to standard H-modes. A higher pedestal pressure in improved H-modes could be an explanation for this. Experiments to clarify this point, which require detailed comparisons of edge profiles in standard and improved H-modes at similar parameters, are planned. It can, however, not be ruled out that the improvement in $H_{98(y,2)}$ is also connected to the density dependence of the ITER-98(y,2) H-mode scaling ($\propto n_e^{0.41}$), often not found in dedicated experiments, or that this scaling does not represent correctly the scaling at rather high values of β_N.

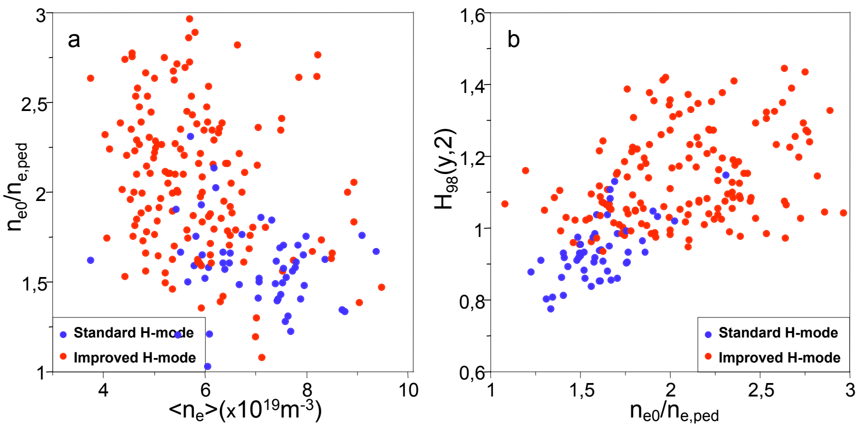

Fig. 5: For data base of Fig. 3 and standard H-modes: (a) density peaking vs. line averaged n_e, (b) H-factor vs. density peaking.

Discharges with peaked densities and no sawteeth often suffer from impurity accumulation. Control of core impurity concentration is therefore an important issue in developing the improved H-mode scenario. High central concentration of high-Z impurities is indeed observed in many improved H-mode discharges heated with NBI only. It has been shown,

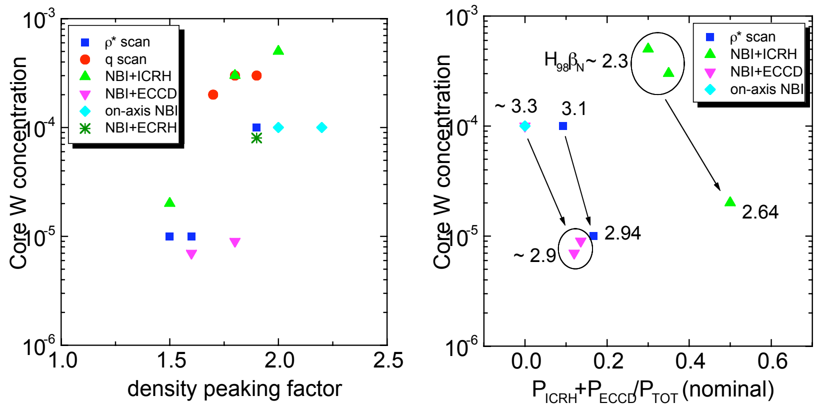

Fig. 6: For selected shots from various improved H-mode studies: Core W concentration vs. density peaking (left) and vs. fraction of central wave heating (right).

however, that low levels of central ECRH (1-1.5 MW) or adding central ICRH with $P_{ICRH} \geq 0.5 \cdot P_{NBI}$ allow to suppress this impurity accumulation [15]. The effect of additional wave heating on central W concentration, density peaking and confinement is further illustrated in Fig. 6 [16]. The core W concentration is reduced by more than an order of magnitude when central wave heating is applied. Concomitantly, the density peaking and to some extent the performance are reduced, the latter, however, in terms of $\beta_N \cdot H_{98(y,2)}$ remains still significantly above standard H-mode values. Similar results are obtained for the core C concentration.

5. MHD Behaviour

As mentioned above, a current density profile with $q_0 \geq 1$ and a low central magnetic shear is a key element of the improved H-mode. MHD activity plays an important role in maintaining this q-profile stationary over periods longer than the current diffusion time (typically ~ 2 s). For the early improved H-modes found on ASDEX Upgrade, (1,1) fishbones were identified to clamp central q at values close to unity [17]. With the off-axis, tangential beams becoming available the parameter range of this scenario was significantly extended. Strong fishbone activity is not present in all of the improved H-mode discharges. As shown in Fig. 2, the amount of off-axis neutral beam driven current together with the bootstrap current are not sufficient to explain the observed current density profile. The small amplitude NTM activity, often present during the high performance phase (see Fig. 7), is the likely candidate responsible for keeping the q-profile stationary, the detailed mechanism, however, is not yet clear.

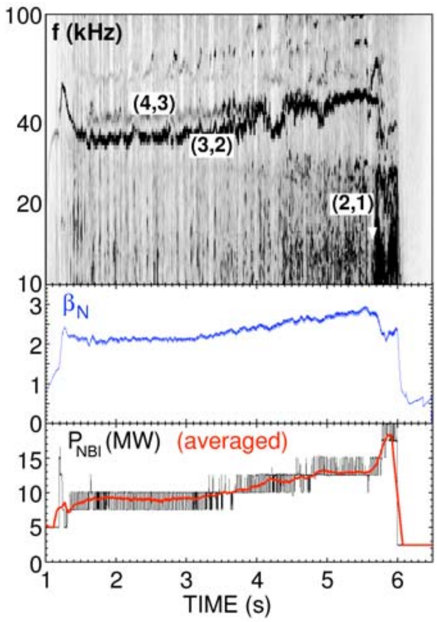

Fig. 7: β-limit (q_{95}=4.3) during power ramp caused by (2,1) mode; top: spectrogram of MHD activity from Mirnov coils; bottom: β_N and NBI power.

The q-profile is thought to be responsible for the benign MHD behaviour of this scenario that allows high-β operation at good confinement. By the avoidance of sawteeth ($q_0 \geq 1$) the main trigger of large amplitude NTMs is removed. It has been pointed out in Ref. [18] that, for high plasma pressures, a low magnetic shear at the (3,2) surface reduces the NTM drive and, consequently, leads to a significantly smaller amplitude of the (3,2) NTM. In addition higher m-number activities are destabilized which could, via non-linear mode coupling, further reduce the amplitude of this mode. Small amplitude (3,2) NTM together with higher m-number mode activities are often seen during the high performance phase of the improved H-mode.

In the course of documenting stationary operation of the low collisionality, improved H-mode at different values of q_{95} (section 3), the maximum attainable β has been assessed as well by continuously ramping up the heating power under feed back control until a severe degradation of confinement is observed. This happened at β_N around 3, almost independently of q_{95}. An example (q_{95} = 4.3) is shown in Fig. 7, which includes a spectrogram of the MHD activity. (3,2) and (4,3) modes are present throughout the power ramp. The maximum β, however, is limited by the occurrence of a (2,1) mode at 5.6 s that quickly locks and causes a strong reduction of plasma pressure despite the fact the heating power is strongly increased. The mode locking, however, does not lead to a major disruption. Generally, improved H-mode plasmas have a very low probability to disrupt. Major disruption have only be seen in cases where a strong central impurity rise is causing the plasma collapse.

6. Improved H-Mode with dominant central ICRH

The experimental results presented so far were obtained with dominant NBI heating. This implies preferential ion heating ($T_i > T_e$) as well as input of momentum and particles which is in contrast to α-heating in a reactor-type plasma. Central wave heating is therefore more reactor relevant. Experiments have been started to establish improved H-modes with dominant central ICRH heating. In these shots, the NBI was feed back controlled to keep β_{pol} at a preset value while the RF power is increased in several steps up to the maximum available power (<7 MW). An example is given in Fig. 8. For the discharge shown a stationary value of β_N = 2.6 was maintained at a confinement factor of $H_{98(y,2)}$ ~ 1.2, even though the density profile in this case is rather flat. For a pulse length of 2 s, P_{ICRH} = 6 MW exceeds P_{NBI} ~ 4.5 MW. The lower traces in Fig. 8 again illustrate the suppression of central W concentration by central heating as discussed in section 4. Since more than 70% of the ICRH power is deposited inside ρ = 0.3, the plasma core is dominated by RF heating. Under the conditions of these experiments (H-minority ~ 6-10%), however, ion heating by ICRH is stronger than electron heating. Nevertheless, the power to the electrons for this combined (ICRH + NBI) heating rises to 1 MW inside ρ = 0.3, compared to 0.4 MW in a comparable NBI only case. The discharge shown in Fig. 8, therefore, has significant core electron heating. By applying strong ICRH, T_i/T_e is strongly reduced. At moderate densities (~$5\cdot10^{19}$ m^3) and q_{95} = 3.8, it changes from $T_i/T_e(0)$ ~ 1.5 for NBI only to close to unity for P_{ICRH} ~ P_{NBI} with no significant effect on the confinement. In summary, the improved H-mode could be established with dominant RF heating in the core, but so far restricted to $P_{ICRH}/P_{NBI} \leq 1.3$ due to the limited ICRH power. Similarly, $T_i/T_e(0)$ has been varied by applying central (ECRH) with $P_{ECRH} \leq 1.6$ MW at q_{95} ~ 4.5, n_e ~ $6\cdot10^{19}$ m^{-3} and β_N ~ 2.6 without affecting the confinement.

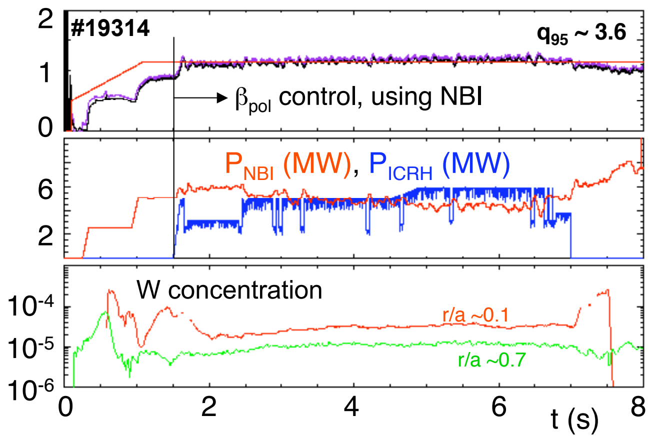

Fig. 8: Example of improved H-mode with dominant ICRH; stationary β_p by feed back control of NBI power with $H_{98(y,2)}$=1.2 and β_N=2.6 at q_{95}=3.6. Low central W concentration during RF heating.

7. Summary

The improved H-mode developed on ASDEX Upgrade combines improved confinement ($H_{98(y,2)}$ >1) with high stability (β_N > 2.5) in stationary discharges, i.e. longer than $40 \cdot \tau_E$ or more than twice the current diffusion time. Its characteristic q-profile, a low central magnetic shear with $q_0 \geq 1$, is obtained by early heating during the current ramp. High performance discharges of this kind have been established over a wide range of q_{95} ($3.2 < q_{95} < 4.5$) and densities up to $0.85 \cdot n_{GW}$. At $q_{95} \sim 3 - 3.5$, a figure of merit for fusion gain, $H_{98(y,2)} \cdot \beta_N / q_{95}^2 \sim 0.3$ was achieved which exceeds the corresponding design value for the ITER baseline scenario by 50%. This ITER value is met at q_{95} around 4 which extrapolates to an improved H-mode operation in ITER at a reduced plasma current and, therefore, an extended pulse length without loss in performance. As far as dimensionless plasma parameters are concerned, the collisionalities, ν^*, in low density improved H-modes on ASDEX Upgrade are rather close to the expected ITER value. The normalized Larmor radii, ρ_i^*, are necessarily above those of ITER but within the range covered by ASDEX Upgrade, no change in the achievable performance is observed. Transport analyses of improved H-modes indicate that core heat transport is governed by ITG/TEM turbulence as it is the case in standard H-mode. The increase in confinement with respect to the H-mode scaling (ITER-98(y,2)) is not fully explained by the stronger peaked density profiles. Effective impurity control by adding central wave heating has been demonstrated. The q-profile of the improved H-mode plays a key role for the high stability: $q_0 \geq 1$ avoids sawteeth as trigger of large NTMs and the low central shear reduces the amplitude of the (3,2) modes present during the high-β phase to a level that their effect on the confinement remains small. The stability is eventually limited at $\beta_N \sim 3$ by the occurrence of a (2,1) mode resulting in an severe degradation of confinement. In view of the application of improved H-modes in reactor-type plasmas, the compatibility of this scenario with high edge densities and low amplitude type-II ELMs, a non-inductive current fraction of up to 50%, as well as its demonstration with $P_{ICRH} > P_{NBI}$, i.e. significant core electron heating, are important issues. In summary, the results presented in this paper establish the improved H-mode as a candidate for a long pulse ITER operation – a "hybrid" of the non-inductive, reversed shear scenario with ITBs and the standard H-mode baseline scenario.

References

[1] ITER Physics Basis, Nucl. Fusion **39** (1999) 2137
[2] Gruber, O. et al., Phys Rev Letters, **83** (1999) 1787
[3] Wade, M. R. et al., 29th EPS Conf. (Montreux 2002), ECA Vol. **26B**, O-2.08
[4] Sips, A. C. C. et al., 30th EPS Conf. (St. Petersburg 2003), ECA, Vol. **27A**, O-1.3A
[5] Kamada, Y. et al., Nucl. Fusion **39** (1999) 1845
[6] Sips, A. C. C. et al., Plasma Phys. Control. Fusion **44** (2002) B69
[7] Pereverzev et al., 1991, IPP-Report, IPP 5/42
[8] Na, Y.-S. et al., Plasma Phys. Control. Fusion **44** (2002) 1285
[9] Angioni, C. et al., Nucl. Fusion **44** (2004) 827
[10] Gruber, O. et al, Nucl. Fusion **41** (2001) 1369
[11] Na, Y.-S. et al., 31th EPS Conf. (London 2004), ECA Vol. **28G**, P-4.125
[12] Luce, T. C. et al., Nucl. Fusion **43** (2003) 321
[13] Manini, A. et al., Plasma Phys. Control. Fusion **46** (2004) 1723
[14] Angioni, C et al., Phys. Rev. Lett. **90** (2003) 205003
[15] Dux, R et al., this conference, EX / P6-14
[16] Maggi, C. F. et al, 31th EPS Conf. (London 2004), ECA Vol. **28G**, P-4.119
[17] Günter, S. et al., Nucl. Fusion **39** (1999) 1535
[18] Günter, S. et al., Nucl. Fusion **44** (2004) 524